Seasonal and interannual variability of elemental carbon in the snowpack of Storglaciären, northern Sweden

Susanne INGVANDER,[1] Gunhild ROSQVIST,[1] Jonas SVENSSON,[2] Helen E. DAHLKE[1]

[1]*Department of Physical Geography and Quaternary Geology, Stockholm University, Stockholm, Sweden*
E-mail: susanne.ingvander@natgeo.su.se
[2]*Climate Change Unit, Finnish Meteorological Institute, Helsinki, Finland*

ABSTRACT. We studied the variability of elemental carbon (EC) over 3 years (2009–11) in the winter snowpack of Storglaciären, Sweden. The goal of this study was to relate the seasonal variation in EC to specific snow accumulation events in order to improve understanding of how different atmospheric circulation patterns control the deposition of EC. Specifically, we related meteorological parameters (e.g. wind direction, precipitation) to snow physical properties, EC content, stable-isotope $\delta^{18}O$ ratios and anion concentrations in the snowpack. The distribution of EC in the snowpack varied between years. Low EC contents corresponded to a predominance of weather systems originating in the northwest, i.e. North Atlantic. Analysis of single layers within the snowpacks showed that snow layers enriched in heavy isotopes coincided predominantly with low EC contents but high chloride and sulfate concentration. Based on this isotopic and geochemical evidence, snow deposited during these events had a strong oceanic, i.e. North Atlantic, imprint. In contrast, snow layers with high EC content coincided with snow layers depleted in heavy isotopes but high anion concentrations, indicating a more continental source of air masses and origin of EC from industrial emissions.

INTRODUCTION

The Earth's radiation budget and climate system depend on the amount of energy absorbed at the Earth's surface (Lemke and others, 2007). Snow- and ice-covered areas have a high reflectivity, or so-called albedo, that limits the absorption of solar radiation. Albedo is the percentage of incoming solar radiation (0.1–15 μm) reflected by the Earth's surface (Ahrens, 1999). The albedo of a snow surface depends on the particle size and shape of snow crystals, the snow density and impurities within a snowpack (Wiscombe and Warren, 1980; Warren, 1982). For example, dust and black carbon (BC) can lower the albedo and lead to greater energy absorption (Warren and Wiscombe, 1980; Clarke and Noone, 1985; Hansen and Nazarenko, 2004).

BC, in particular, has an amplifying effect on the melt rate of a snowpack as it increases the absorption of solar radiation (Flanner and others, 2007). Originating from both natural and anthropogenic combustion sources, BC is typically deposited onto the snow surface through wet or dry deposition. However, knowledge of the primary sources and processes involved in the transport and deposition of BC, its temporal and spatial variability and implications for post-depositional processes within snow are limited. In addition, most studies on spatial variability of BC in snow are limited to snow surveys from the Arctic (e.g. Forsström and others, 2009; Doherty and others, 2010) or temporal variability of BC in snow and ice cores from the Greenland ice sheet (McConnell and others, 2007) and the Himalaya (e.g. Ming and others, 2008; Cong and others, 2009; Xu and others, 2009; Kaspari and others, 2011; Wang and others 2012).

Here we present results from a study of the seasonal and interannual variability in elemental carbon (EC) content in a winter snowpack on Storglaciären, northern Sweden. Defined operationally by the analysis technique, EC is generally used synonymously with BC. Both terms refer to the refractory and light-absorbing properties of carbonaceous aerosols. In this paper, we use the term EC, as a thermal/optical method was applied. We study the EC content and its relation to snow physical and geochemical parameters. We compare the snow EC content, physical and geochemical data to meteorological data from two automatic weather stations (AWS), located at the Tarfala Research Station (TRS; 67°55′ N, 18°37′ E; 1135 m a.s.l.) and in Katterjokk, provided by the Swedish Meteorological and Hydrological Institute (SMHI) (Fig. 1), in order to identify different snow layers and relate their differences in EC and snow chemistry to regional weather patterns and potential pollution sources. Our hypothesis is that North Atlantic air masses, with a trajectory from the north, northwest or west, contain less EC and are characterized by ^{18}O-enriched precipitation compared to continental air masses from the northeast, east, southeast or south. This is because the industrial pollution load in air masses from eastern Fennoscandia (including nearby Kiruna) and Russia is larger (Hegg and others, 2009).

METHODS

Study site

The sampling site is located on Storglaciären, which is situated in the Tarfala valley, east of Kebnekaise mountain, northern Sweden. The snow-pit site is located at 1520 m a.s.l. (Fig. 1) on a relatively flat part of the Storglaciären accumulation area between the north and south cirques (Fig. 1). The high alpine Tarfala valley is situated in the Scandinavian mountains, a northeast–southwest oriented mountain range that functions as a climate divide between the maritime west and the continental east (Holmlund and Jansson, 1999). Tarfala valley is characterized by high accumulation rates since the site is relatively sheltered, which reduces mixing in the snowpack and wind transportation. The mean annual temperature at TRS is –3.5°C (1965–2011); the mean annual precipitation measured at TRS is 1997 ± 450 mm a^{-1} (Dahlke and others, 2012). Most of the winter precipitation originates

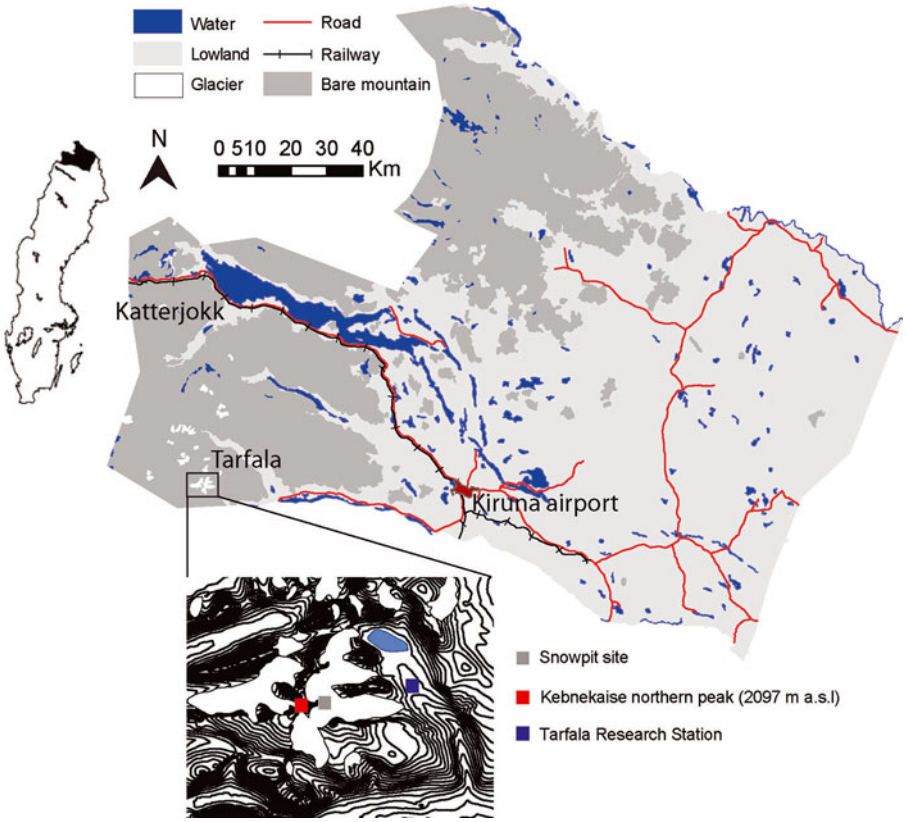

Fig. 1. Map of the study area showing the location of the snow pit on Storglaciären within the Tarfala research catchment and SMHI automatic weather stations near the Tarfala Research Station and Katterjokk in northern Sweden.

from North Atlantic air masses during low-pressure passages (Busuioc and others, 2001). The highest wind speeds occur when the general (>2000 m a.s.l.) wind direction is westerly or northwesterly.

Snow sampling and estimation of snow physical parameters

Snow samples were collected at the end of the accumulation period, in April of 2009, 2010 and 2011. The seasonal snow depth during these years was 285–380 cm (Table 1). Snow sampling and measurements of snow physical parameters were performed along the south wall of a pit dug down to the previous summer surface. Data on the EC content, stable water isotopic composition and snow density were available for all three years. Snow sampling to estimate the EC content was conducted at an increment of 50, 9 and 25 cm in 2009, 2010 and 2011, respectively, while snow density was estimated every 25, 3 and 5 cm in these years. Snow samples for stable water isotope analysis were taken every 10, 3 and 5 cm in 2009, 2010 and 2011, respectively. In 2009, additional samples for analysis of chloride (Cl^-), sulfate (SO_4^{2-}) and nitrate (NO_3^-) concentrations were taken at a sample resolution of 10 cm. In 2010, additional snow physical parameters (e.g. snow temperature, permittivity, stratigraphy and snow particle size) were determined. On site, a PT100 instrument was used to register the snow temperature; the snow density was estimated based on the volume and weight of each sample and also using a TOIKKA AS snow fork to determine the density and permittivity of the snowpack (Shivola and Tiuri, 1986). The stratigraphy was described and the snow particle size was determined using the digital snow particle property (DSPP) method (Ingvander and others, 2012).

For chemical and isotope analysis, snow samples were stored hermetically in plastic bags until laboratory analysis on the same day at TRS. Samples for analysis of the isotopic composition and Cl^-, SO_4^{2-} and NO_3^- concentrations were slowly melted in the sealed plastic bags at 4°C at TRS. Snowmelt water was bottled in 50 mL HDPE bottles with poly-seal caps until laboratory analysis at Stockholm University. Samples were analyzed for $^{18}O/^{16}O$ ratio and $^{2}H/^{1}H$ content (expressed as $\delta^{18}O$ and δd) using a laser absorption spectrometer (Liquid-Water Isotope Analyzer DLT-100, Los Gatos Research Inc., Mountain View, CA, USA) with a precision of 0.15‰ and 0.6‰ for $\delta^{18}O$ and δd, respectively. These $\delta^{18}O$ and δd contents are reported in per mil relative to Vienna Standard Mean Ocean Water (VSMOW). Analysis of Cl^-, SO_4^{2-} and NO_3^- concentrations was performed using a Dionex IC25 ion chromatograph at Stockholm University. Snow samples for the EC analysis

Table 1. Summary of the sampling campaigns at the snow-pit site (Fig. 1) and the average soot content, mean $\delta^{18}O$ isotopic composition and mean density for each year

Parameter	2009	2010	2011
Date	16 April	14 April	4 April
Depth (cm)	390	300	268
Average soot content conc. (μg L^{-1})	15.26 ± 10.25	10.29 ± 8.07	6.90 ± 4.04
Average $\delta^{18}O$ (‰)	−14.92 ± 3.55	−15.09 ± 3.55	−16.12 ± 2.75
Average density (g cm^{-3})	0.45 ± 0.09	0.40 ± 0.08	0.36 ± 0.07

Table 2. Snow accumulation season (SAS) divided into four periods based on time of year: SAS1: start of SAS to October; SAS2: November–December; SAS3: January–February; and SAS4: March to end of SAS. The table shows the dates of each SAS, the mean temperature, wind speed and major wind direction during the SAS periods

	SAS1			SAS2			SAS3			SAS4		
	2009	2010	2011	2009	2010	2011	2009	2010	2011	2009	2010	2011
Time-span	29 Sep–31 Oct	23–31 Oct	9–31 Oct	1 Nov–31 Dec	1 Nov–31 Dec	1 Nov–31 Dec	1 Jan–28 Feb	1 Jan–28 Feb	1 Jan–28 Feb	1 Mar–14 May	1 Mar–13 May	9 Apr–5 Jun
Temperature (°C)	–2.8	–3.2	–4.5	–7.7	–8.9	–9.6	–11.3	–11–28	n.a.	–7.7	–8.4	–1.0
Wind speed ($m\,s^{-1}$)	8.7	5.4	10.6	11.2	5.9	7.8	9.8	7.3	n.a.	8.3	9.1	4.4
Wind direction (°)	324	324	309	331	332	333	327	332	n.a.	326	325	327

were extracted from the snow pit and kept frozen until filtration. The snow was melted in a glass jar in a microwave oven and filtered through a microquartz filter according to the methods of Forsström and others (2009) and Aamaas and others (2011). Dried filters were analyzed in a Thermal/Optical Carbon Aerosol Analyzer (OCEC). Detailed descriptions of the instrument and the analysis protocol (EUSAAR_2) are given by Birch and Cary (1996) and Cavalli and others (2010), respectively.

Using the filtration method introduces an underestimate of the EC concentration in the snow sample, as some particles may percolate through the filter and not be accounted for during OCEC analysis. This filtering deficiency, also known as undercatch, has been proposed to be in the order of 15–50% (Ogren and others, 1983; Doherty and others, 2010) depending on the type of filter used. In this paper, undercatch was measured by having two filters on top of each other during filtration. For the subset of 14 samples to which this evaluation was applied, an undercatch of roughly 50% existed. This is probably a high estimate, as Aamaas and others (2011) had a much lower undercatch (undetectable amounts) when using identical filters. Further experiments are needed before solid conclusions on undercatch for microquartz filters can be drawn. It does, however, provide insight into the uncertainty and underestimation present in our EC dataset.

Another possible loss of EC particles using the filter method is by particles attaching to the glass walls of jars used to melt the snow sample (Ogren and others, 1983; Clarke and Noone, 1985). This was investigated by Forsström and others (2009) who concluded that EC particles were lost when a liquid sample was stored for longer than 1.5 days in a glass jar. This was not the case for any of the samples filtered in this study.

Meteorological and snow accumulation data

The meteorological parameters wind speed, wind direction and air temperature, available with a temporal resolution of 10 min, were used. They were recorded at an AWS located near TRS ~3 km east of the snow pit at 1150 m a.s.l. (67°54′44″ N, 18°36′46″ E) and are provided by SMHI. In order to better estimate the regional meteorological conditions during the study period, we included additional meteorological data from an SMHI weather station situated in Katterjokk near Abisko (68°21′ N, 18°10′ E; 500 m a.s.l.). We used meteorological data collected during the snow accumulation season (SAS; Shulski and others, 2004), the period when temperature is continuously negative and precipitation therefore falls as snow. In addition, we used the SMHI definition of the onset of winter as the first day of a 5 day period with daily mean air temperatures at or below 0°C. Similarly the end of winter was determined as the first day of a 5 day period with the mean air temperature above 0°C. We further divided the SAS into four periods (SAS1: start of SAS to October; SAS2: November–December; SAS3: January–February; and SAS4: March to end of SAS). SAS1 and SAS4 vary in length since the total season length differs over time (Table 1). Snow accumulation was estimated based on precipitation data ($mm\,h^{-1}$) available from Katterjokk AWS and provided by SMHI. Winter precipitation data were not available for Tarfala AWS.

RESULTS

Meteorological conditions and snow accumulation

The mean winter temperature decreased over the 2009–11 study period (Table 2). Figure 2 shows the wind speed and wind direction for both the Tarfala and Katterjokk AWS. Wind speeds measured at Tarfala and Katterjokk were similar during the SAS1–2 periods during all three years. However, in 2009 the wind speed observed at Katterjokk was three times smaller than recorded at Tarfala. Over the study period, the highest wind speeds were observed at Tarfala in the first part of winter 2009 (SAS1–2). In 2010 and 2011, wind speeds were consistently lower in late winter (SAS3–4). The predominant wind direction observed at Tarfala was west-northwest to northwest during all SAS periods and years. Wind directions recorded at Katterjokk showed a greater range, reflecting that station's more open setting (Fig. 2).

The bulk snow accumulation on Storglaciären during the 2009, 2010 and 2011 winters was 390, 300 and 268 cm, respectively. However, in all three years the majority of snow was accumulated in SAS3 (January–February). These values compare to a total winter mass balance of 2.02, 0.91 and 1.32 m w.e. for 2009, 2010 and 2011, respectively. The mean snow density decreased from $0.45\,g\,cm^{-3}$ to $0.36\,g\,cm^{-3}$ over the 3 year sampling period (Table 1; Fig. 2). The decrease in snow accumulation rate at Tarfala from 2009 to 2011 is consistent with precipitation amounts recorded at Katterjokk, which showed a decrease in total snow accumulation for the SAS from 2009 to 2011 (Fig. 3).

Snow chemistry

During the 2009–11 study period, the bulk EC content varied between 0 and $30.4\,mg\,L^{-1}$. However, the average EC content decreased from 15.3 to $6.9\,\mu g\,L^{-1}$. As indicated by the standard deviation, 2011 showed the smallest variability in

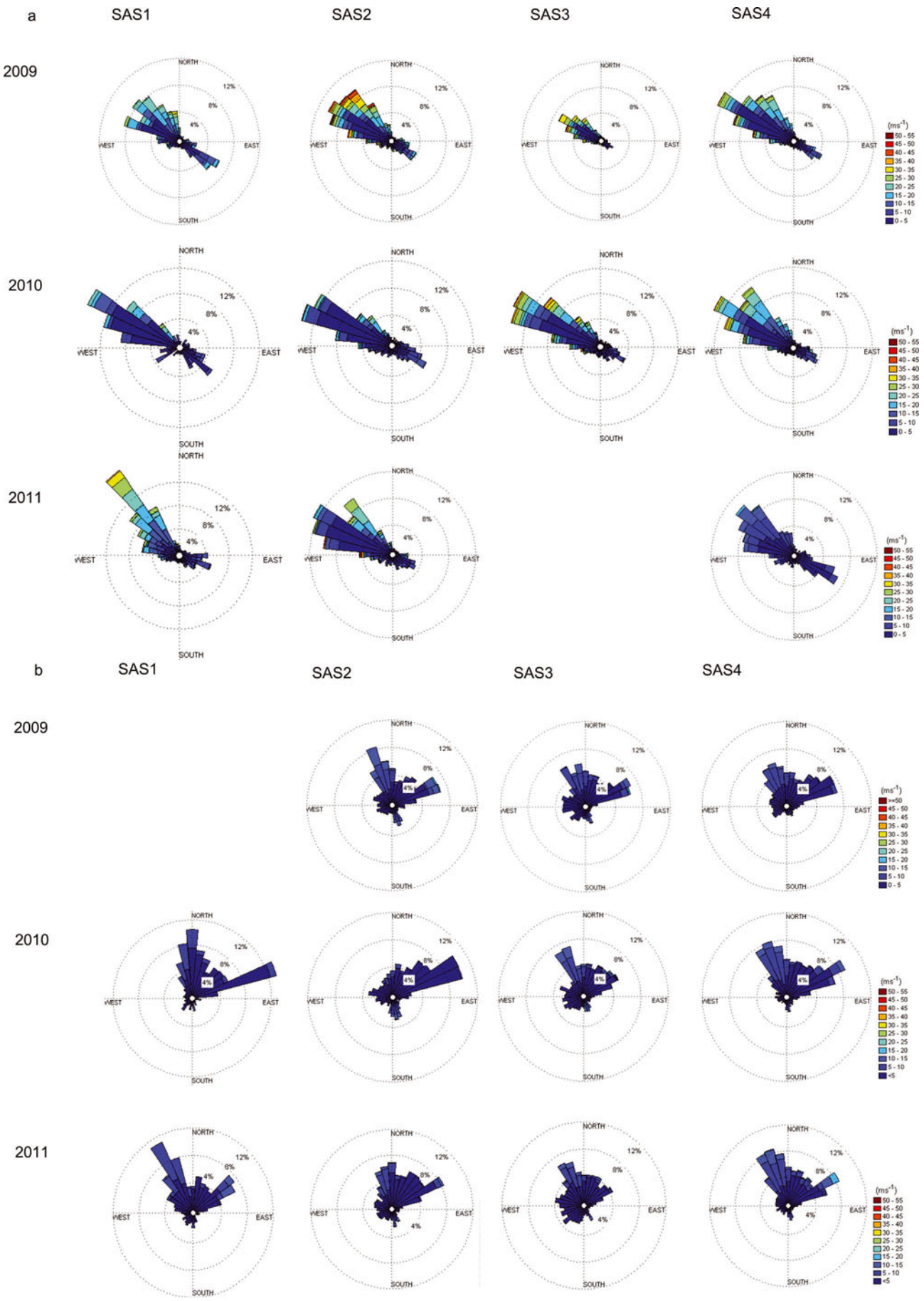

Fig. 2. The major wind directions measured at Tarfala AWS (a) and Katterjokk (b) in 2009, 2010 and 2011. Data are shown for the following snow accumulation seasons: SAS1 (start of SAS to October), SAS2 (November–December), SAS3 (January–February) and SAS4 (March to end of SAS). The wind direction is indicated by the direction of each spoke; the wind speed is indicated by the length and color of each spoke emanating from the center of the circle.

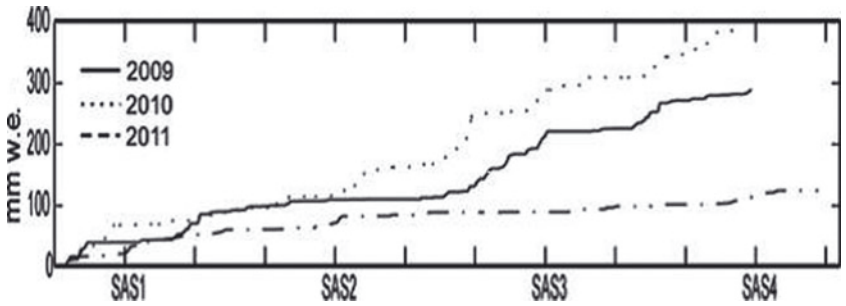

Fig. 3. Snow accumulation measured at Katterjokk AWS for SAS1–4, 2009–11.

EC content within the snowpack. In 2009, higher EC concentrations were measured in the upper part (upper 150 cm) of the snowpack, while in 2010 and 2011 higher EC concentrations were observed in the lower part (Fig. 4). The relatively high EC contents at the base of the 2009 and 2010 snowpack suggest that mixing occurred between the early-winter snow and the previous summer surface, which is typically characterized by high EC content due to continuous deposition of soot over the summer (Xu and others, 2012).

Snow $\delta^{18}O$ ratios varied between –9.68‰ and –25.56‰ over the study period. The snowpack weighted mean average $\delta^{18}O$ value for 2009, 2010 and 2011 was –14.9‰, –15.1‰ and –16.1‰, respectively, indicating that the snowpack became isotopically more depleted from 2009 to 2011 (Table 1). In comparison, the 1961–90 long-term average $\delta^{18}O$ value measured in precipitation in Kiruna was –15.7‰ (GNIP (global network for isotopes in precipitation) database 2012). However, variability in $\delta^{18}O$ ratios was greatest in 2010, when four events with decreased $\delta^{18}O$ values can clearly be identified (Fig. 4).

A comparison of the $\delta^{18}O$ ratios with the EC content in the 2010 snowpack shows that snow layers depleted in

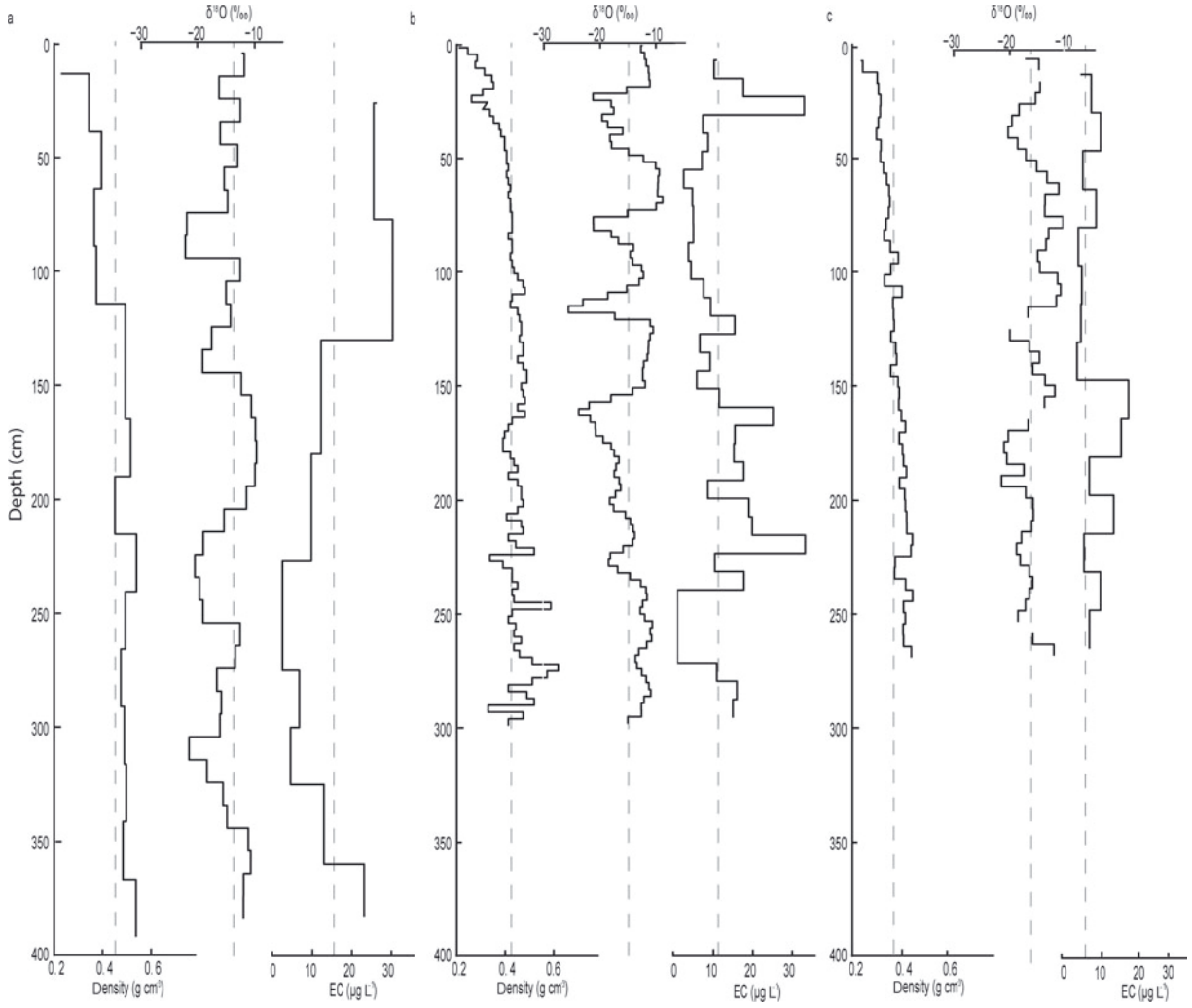

Fig. 4. Density (g cm^{-3}), isotopic composition ($\delta^{18}O$; ‰) and EC concentrations (µg L^{-1}) in the snow pit in (a) 2009 (b) 2010 and (c) 2011. The density analysis is performed using 25 cm increments in 2009, 3 cm in 2010 and 5 cm in 2011. The isotope analysis is performed with 10 cm increments in 2009, 3 cm in 2010 and 5 cm in 2011. The BC samples are analyzed with 50 cm increments in 2009, 8 cm in 2010 and 25 cm in 2011.

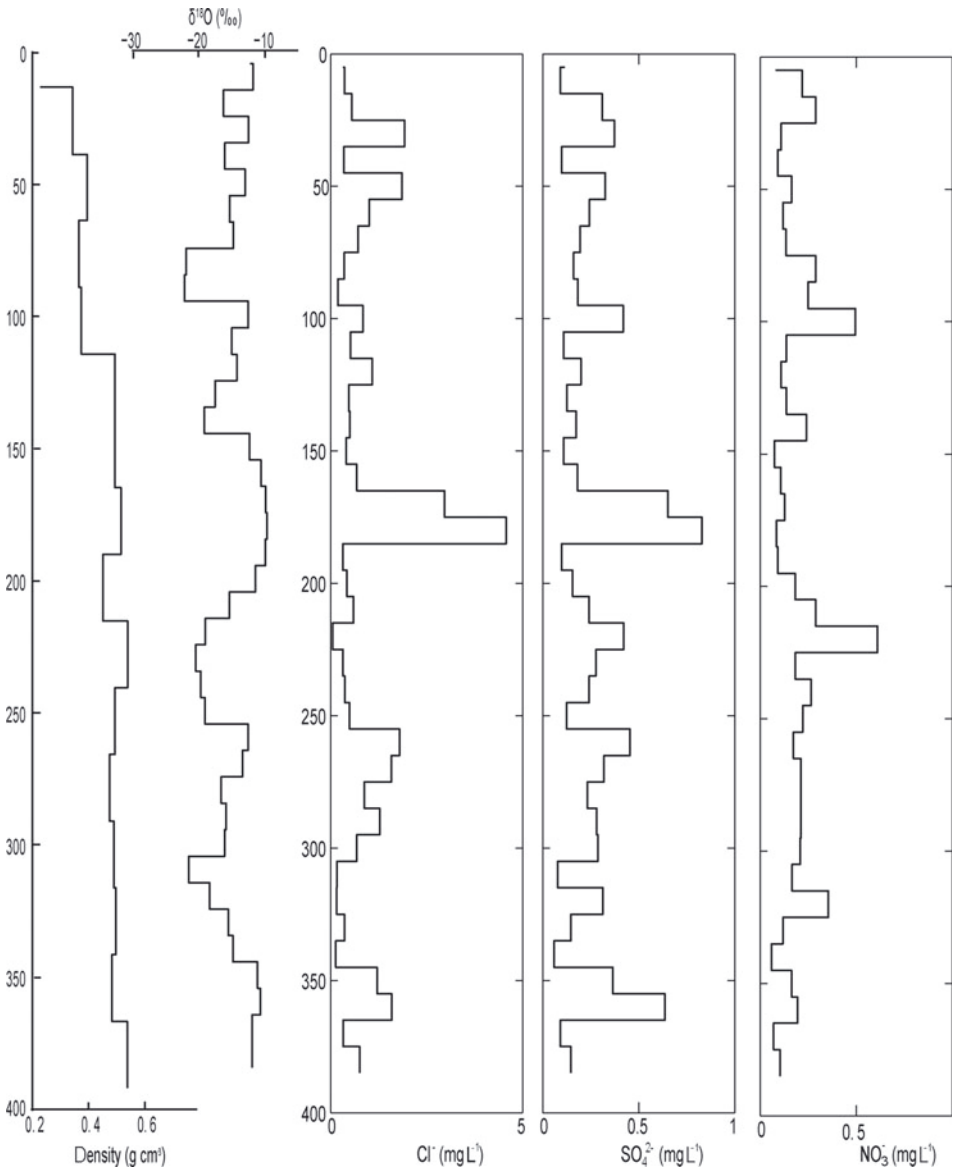

Fig. 5. The $\delta^{18}O$ stratigraphy in the snowpack in 10 cm increments correlated to the chemical elements in the snowpack: chloride (Cl^-), sulfate (SO_4^{2-}) and nitrous oxide (NO_3).

heavy isotopes coincided with layers showing elevated EC contents. This pattern can also be detected in the 2009 and 2011 profiles, but is less pronounced due to the lower sample resolution (especially in 2009). The Cl^-, SO_4^{2-} and NO_3^- concentrations measured in the 2009 snowpack ranged between 0.047 and 4.57, 0.058 and 0.611, and 0.059 and 0.61 mg L^{-1}, respectively. High Cl^- and SO_4^{2-} concentrations occurred at 365, 265 and 185 cm depth and coincided with snow layers enriched in heavy isotopes but with low EC content (Fig. 5). As shown in Figure 6, the variability in snow density, conductivity and the presence of ice layers in the 2010 snowpack resemble the variation in EC content. For example, the higher EC content observed at 240 cm depth coincided with an ice layer.

DISCUSSION

Several processes are involved in the deposition of EC onto a snowpack surface. EC particles can either be directly deposited onto the snow surface via dry deposition (Hansen and others, 2004) or washed out from the atmosphere (scavenged) with precipitation (Warren and Clarke, 1990; Hadley and others, 2010; Schwikowski and Eichler, 2010). Since EC particles can act as nuclei in cloud formation they can be deposited as part of the snow accumulation (Jacobson, 2006). As shown in Figure 4, the 2010 and 2011 snowpacks showed higher EC content in the lower 100–150 cm, while the 2009 snowpack showed higher EC content in the uppermost 150 cm of the snowpack. The early-winter season was windier in 2009 than in 2010 and 2011 (Fig. 2a and b), suggesting that EC deposition shown by concentration does not primarily occur during events with high wind speeds. As higher wind speeds are usually associated with passages of North Atlantic weather systems, this implies that air masses originating from the North Atlantic deposit less EC than Arctic or continental air masses.

Variability in $\delta^{18}O$ can be used to infer different precipitation events with different precipitation sources within a snowpack (Sinclair and Marshall, 2009; Lafrenière and Sinclair, 2011). This is because the $\delta^{18}O$ ratio of precipitation depends on the condensation temperature (the lower the temperature, the more depleted the snow in heavy

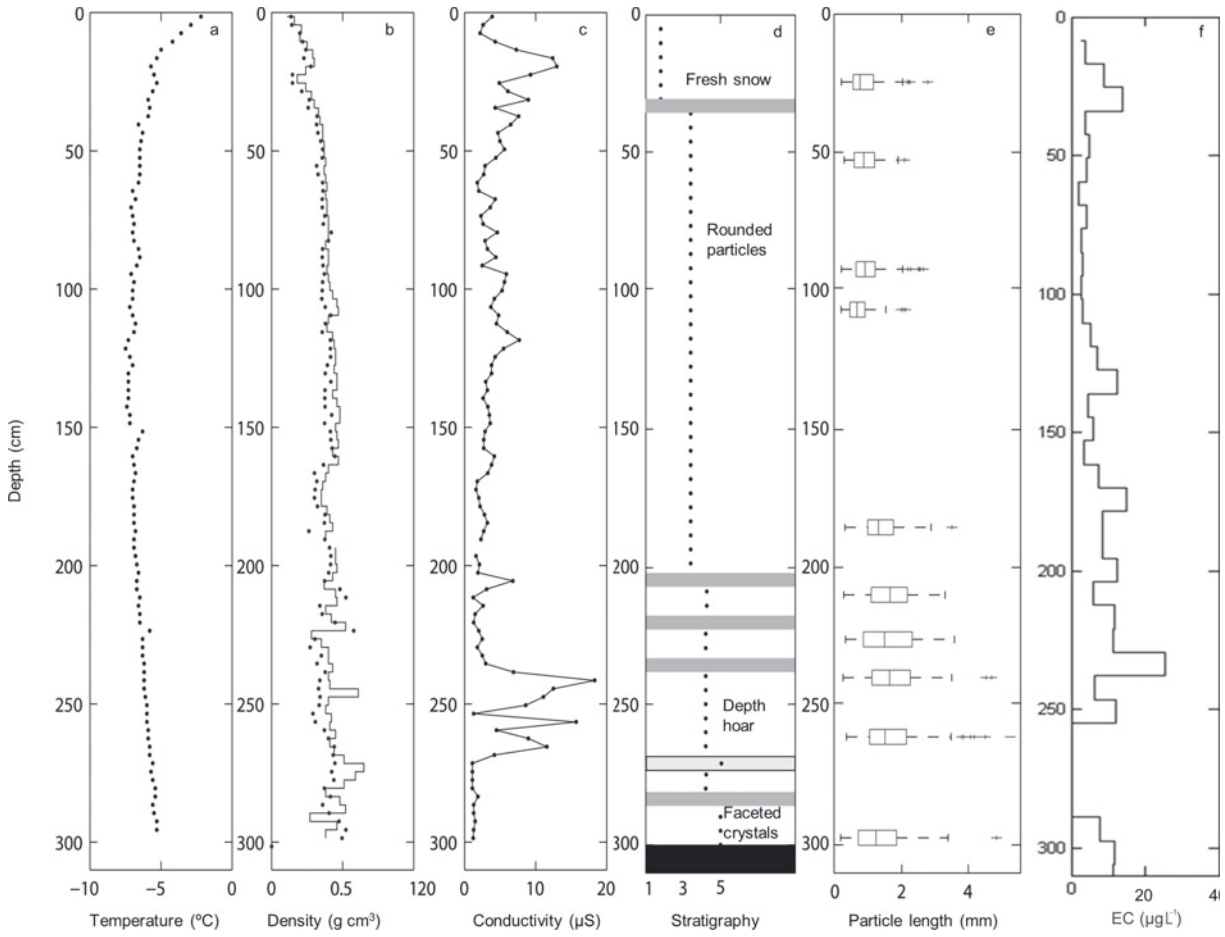

Fig. 6. Physical parameters retrieved from the snow pit in 2010: (a) temperature sampled by PT100; (b) density sampled manually by weighing samples with 3 cm increments (solid line) and using the snow fork with 3 cm resolution (dots); (c) electrical conductivity measurements using the snow fork with 3 cm resolution; (d) stratigraphy based on manual observation and (e) the particle sizes determined using the DSPP method (Ingvander and others, 2012); and (f) EC sampled with 8 cm increments and analyzed in the OCEC instrument, and the concentrations calculated based on the sample volume.

isotopes) and the source and trajectory of the air masses. For example, precipitation originating from the North Atlantic (i.e. maritime source) is typically more enriched in ^{18}O compared to air masses from the north (i.e. arctic regions) or continental east (Bowen and Wilkinson, 2002). During the study period the mean weighted average $\delta^{18}O$ of the snowpack became isotopically more depleted, which could reflect the lower winter air temperatures observed in 2010 and 2011. However, when comparing EC content to the isotopic composition within each profile, a switch in the correspondence of both parameters is apparent. In the upper parts of all three snowpacks, snow layers depleted in heavy isotopes coincided predominantly with high EC contents, while, in the lower parts, snow layers enriched in heavy isotopes coincided with high EC contents. This dynamic suggests that isotopic redistribution and fractionation has occurred in the snowpacks, as reflected by the general increase in $\delta^{18}O$ when moving from the surface to the bottom of the snowpack. This discrepancy in the correspondence between $\delta^{18}O$ and EC content, especially in the lower parts of the snowpack, might be caused by the enrichment in heavy isotopes within the profile due to sublimation/evaporation or transport of lighter isotopes by meltwater within the profiles, while the EC particles remained immobile. However, it can be speculated that some of the ^{18}O enrichment in the lower parts of the snowpacks might be accelerated by the higher EC contents, leading to increased absorption of solar radiation and hence increased warming of the snowpack. In contrast, the correspondence of snow layers depleted in heavy isotopes in the upper parts of the snowpacks with layers characterized by high EC contents suggests that air masses originating from the north, northeast, east and southeast, which are typically more depleted in heavy isotopes, contain greater EC loads. This is expected, as the potential sources of EC (e.g. the industrial area of Kiruna) are located along the trajectories of air masses from these directions.

These results can be further corroborated with the Cl^-, SO_4^{2-} and NO_3^- concentrations measured within the 2009 snowpack. In 2009 we noted three events where concentrations of both Cl^- and SO_4^{2-} were increased, suggesting that precipitation had a strong oceanic, i.e. North Atlantic, imprint (Lafrenière and Sinclair, 2011). Air masses originating from oceanic sources can have high concentrations of Cl^-, which is produced from ocean spray that acts as nucleation source in precipitation build-up (Davidson and others, 1989). In contrast, SO_4^{2-} can have multiple sources such as sea spray, volcanic gases, biological decay or human activity (Delmas and Boutron, 1978). Since it peaked at the same depth as Cl^- in our analysis, we assume that it is of oceanic origin. This is corroborated by the $\delta^{18}O$ ratios observed during these events. As expected, snow layers characterized

by high chloride and sulfate concentrations coincided with snow layers enriched in ^{18}O, which confirms a North Atlantic source of the precipitation (or a relatively warmer air mass).

The observed isotopic, geochemical and EC data suggest potential post-depositional changes in EC concentrations in the snow. For example, in the 2010 snowpack an ice layer was detected at the same depth (240 cm) as a snow layer with increased EC content (Fig. 4). An explanation for the development of this ice layer could be a precipitation event with rain (with a high EC content) or a melt event concentrating EC. Another explanation could be that high wind speeds compacted the snow and created a glazed surface (ice surface), compacted the snow particles and thereby led to an increase in EC content (Jaedicke and others, 2000). Larger particle sizes would be reflected by increased density in the snowpack. Increased amounts of EC in the snow could induce immediate melt in the snowpack by absorbing greater amounts of solar radiation or ground heat flux (Clarke and Noone, 1985; Grenfell and others, 1994). The induced melt would result in larger snow particles within the snowpack due to mobility of moist air or water, which is visible both in the stratigraphy of the snowpack and the snow particle sizes shown in Figure 4.

CONCLUSIONS

We have presented a comparative analysis of the variability in EC, stable water isotopic composition and snow physical parameters in a winter snowpack on Storglaciären over 3 years (2009–11). The isotopic and geochemical data in each snowpack were compared to meteorological parameters in order to relate the seasonal variation in EC to specific snow accumulation events and atmospheric sources of EC. The bulk EC content and weighted mean $\delta^{18}O$ values in the snowpack on Storglaciären decreased over the 3 year study period. However, the distribution of BC in the snowpack varied between years. The 2009 snowpack showed higher EC content in the upper half of the profile, while the 2010 and 2011 profiles showed higher EC content in the lower half. When EC content was compared to isotopic composition within each profile, a switch in the correspondence of both parameters was apparent. In the upper parts of all three snowpacks, snow layers depleted in heavy isotopes coincided predominantly with high EC contents, while in the lower parts snow layers enriched in heavy isotopes coincided with high EC contents. This switch can be attributed to isotopic redistribution and fractionation within the snowpack, which causes enrichment in heavy isotopes in the lower parts of the snowpack. However, the geochemical data in the upper parts of the snowpacks, in conjunction with the meteorological data, indicate that snow layers with low EC content corresponded to high chloride and sulfate concentrations and increased $\delta^{18}O$ values, suggesting that snow deposited during these events had a strong oceanic, i.e. North Atlantic, imprint. Thus our results support our hypothesis that the EC load is lower in North Atlantic air masses from the north, northwest and west, compared to continental air masses from the northeast, east, southeast or south.

ACKNOWLEDGEMENTS

This research was partially financed by Metsä Tissue AB environmental research, the Tarfala Research Station, the Department of Physical Geography and Quaternary Geology, Stockholm University, and the Bergström Foundation. We acknowledge the staff who worked in the field retrieving samples, and in the laboratory analyzing EC and chemistry samples.

REFERENCES

Aamaas B, Bøggild CE, Stordal F, Berntsen T, Holmén K and Ström J (2011) Elemental carbon deposition to Svalbard snow from Norwegian settlements and long-range transport. *Tellus B*, **63**(3), 340–351 (doi: 10.1111/j.1600-0889.2011.00531.x)

Ahrens CD (1999) *Meteorology today: an introduction to weather, climate and the environment*, 6th edn. Brooks/Cole Thomson Learning, Belmont, CA

Birch ME and Cary RA (1996) Elemental carbon-based method for monitoring occupational exposures to particulate diesel exhaust. *Aerosol Sci. Technol.*, **25**(3), 221–241 (doi: 10.1080/02786829608965393)

Bowen GJ and Wilkinson B (2002) Spatial distribution of $\delta^{18}O$ in meteoric precipitation. *Geology*, **30**(4), 315–318 (doi: 10.1130/0091-7613(2002)030<0315:SDOOIM>2.0.CO;2)

Busuioc A, Chen DL and Hellstrom C (2001) Temporal and spatial variability of precipitation in Sweden and its links with large-scale atmospheric circulation. *Tellus A*, **53**(3), 348–367

Cavalli F, Viana M, Yttri KE, Genberg J and Putaud J-P (2010) Toward a standardised thermal–optical protocol for measuring atmospheric organic and elemental carbon: the EUSAAR protocol. *Atmos. Measure. Tech.*, **3**(1), 79–89 (doi: 10.5194/amt-3-79-2010)

Clarke AD and Noone KJ (1985) Soot in the Arctic snowpack: a cause for perturbations in radiative transfer. *Atmos. Environ.*, **19**(12), 2045–2053 (doi: 10.1016/j.atmosenv.2007.10.059)

Cong Z, Kang S and Qin D (2009) Seasonal features of aerosol particles recorded in snow from Mt. Qomolangma (Everest) and their environmental implications. *J. Environ. Sci.*, **21**(7), 914–919 (doi: 10.1016/S1001-0742(08)62361-X)

Dahlke HE, Lyon SW, Stedinger JR, Rosqvist G and Jansson P (2012) Contrasting trends in floods for two sub-arctic catchments in northern Sweden – does glacier presence matter? *Hydrol. Earth Syst. Sci.*, **16**(7), 2123–2141 (doi: 10.5194/hess-16-2123-2012)

Davidson CI, Harrington JR, Stephenson MJ, Small MJ, Boscoe FP and Gandley RE (1989) Seasonal variations in sulfate, nitrate and chloride in the Greenland ice sheet: relation to atmospheric concentrations. *Atmos. Environ.*, **23**(11), 2483–2493 (doi: 10.1016/0004-6981(89)90259-X)

Delmas R and Boutron C (1978) Sulfate in Antarctic snow: spatio-temporal distribution. *Atmos. Environ.*, **12**(1–3), 723–728 (doi: 10.1016/0004-6981(78)90253-6)

Doherty S, Warren SG, Grenfell TC, Clarke AD and Brandt RE (2010) Light-absorbing impurities in Arctic snow. *Atmos. Chem. Phys.*, **10**(23), 11 647–11 680 (doi: 10.5194/acp-10-11647-2010)

Flanner MG, Zender CS, Randerson JT and Rasch PJ (2007) Present-day climate forcing and response from black carbon in snow. *J. Geophys. Res.*, **112**(D11), D11202 (doi: 10.1029/2006JD008003)

Forsström S, Ström J, Pedersen CA, Isaksson E and Gerland S (2009) Elemental carbon distribution in Svalbard snow. *J. Geophys. Res.*, **114**(D19), D19112 (doi: 10.1029/2008JD011480)

Grenfell TC, Warren SG and Mullen PC (1994) Reflection of solar radiation by the Antarctic snow surface at ultraviolet, visible, and near-infrared wavelengths. *J. Geophys. Res.*, **99**(D9), 18 669–18 684 (doi: 10.1029/94JD01484)

Hadley OL, Corrigan CE, Kirchstetter TW, Cliff SS and Ramanathan V (2010) Measured black carbon deposition on the Sierra Nevada snow pack and implication for snow pack retreat. *Atmos. Chem. Phys.*, **10**(4), 10 463–10 485 (doi: 10.5194/acpd-10-10463-2010)

Hansen JE and Nazarenko L (2004) Soot climate forcing via snow and ice albedos. *Proc. Natl Acad. Sci. USA (PNAS)*, **101**(2), 423–428 (doi: 10.1073/pnas.2237157100)

Hegg DA, Warren SG, Grenfell TC, Doherty SJ, Larson TV and Clarke AD (2009) Source attribution of black carbon in Arctic snow. *Environ. Sci. Technol.*, **43**(11), 4016–4021 (doi: 10.1021/es803623f)

Holmlund P and Jansson P (1999) The Tarfala mass balance programme. *Geogr. Ann. A*, **81**(4), 621–631 (doi: 10.1111/j.0435-3676.1999.00090.x)

Ingvander S, Johansson C, Jansson P and Pettersson R (2012) Comparison of digital and manual methods of snow particle size estimation. *Hydrol. Res.*, **43**(3), 192–202 (doi: 10.2166/nh.2012.078)

Jacobson MZ (2006) Effects of externally-through-internally-mixed soot inclusions within clouds and precipitation on global climate. *J. Phys. Chem.*, **110**(21), 6860–6873 (doi: 10.1021/jp056391r)

Jaedicke C, Thiis TK and Bank B (2000) The snowdrift pattern around a small hill in the high Arctic. In Hjorth-Hansen E, Holand I, Loset S and Norem H eds. *Snow Engineering: Recent Advances and Developments. Proceedings of the Fourth International Conference on Snow Engineering, 19–21 June 2000, Trondheim, Norway.* A. A. Balkema, Rotterdam, 75–80

Kaspari S and 6 others (2011) Recent increase in black carbon concentrations from a Mt. Everest ice core spanning 1860–2000 AD. *Geophys. Res. Lett.*, **38**(4), L04703 (doi: 10.1029/2010GL046096)

Lafrenière MJ and Sinclair KE (2011) Snowpack and precipitation chemistry at a high altitude site in the Canadian Rocky Mountains. *J. Hydrol.*, **409**(3–4), 737–748 (doi: 10.1016/j.jhydrol.2011.09.007)

Lemke P and 10 others (2007) Observations: changes in snow, ice and frozen ground. In Solomon S and 7 others eds. *Climate change 2007: the physical science basis. Contribution of Working Group I to the Fourth Assessment Report of the Intergovernmental Panel on Climate Change*. Cambridge University Press, Cambridge, 339–383

McConnell JR and 9 others (2007) 20th-century industrial black carbon emissions altered Arctic climate forcing. *Science*, **317**(5843), 1381–1384 (doi: 10.1126/science.1144856)

Ming J and 6 others (2008) Black carbon record based on a shallow Himalayan ice core and its climatic implications. *Atmos. Chem. Phys.*, **8**(5), 1343–1352 (doi: 10.5194/acp-8-1343-2008)

Ogren JA, Charlson RJ and Groblicki PJ (1983) Determination of elemental carbon in rainwater. *Anal. Chem.*, **55**(9), 1569–1572 (doi: 10.1021/ac00260a027)

Schwikowski M and Eichler A (2010) Alpine glaciers as archives of atmospheric deposition. In Bundi U ed. *The handbook of environmental chemistry. Vol. 6: Alpine waters*. Springer, Berlin, 141–150

Shulski MD and Seeley MW (2004) Application of snowfall and wind statistics to snow transport modeling for snowdrift control in Minnesota. *J. Appl. Meteorol.*, **43**(11), 1711–1721 (doi: 10.1175/JAM2140.1)

Sihvola A and Tiuri M (1986) Snow fork for field determination of the density and wetness profiles of a snow pack. *IEEE Trans. Geosci. Remote Sens.*, **24**(5), 717–721 (doi: 10.1109/TGRS.1986.289619)

Sinclair KE and Marshall SJ (2009) Temperature and vapour-trajectory controls on the stable-isotope signal in Canadian Rocky Mountain snowpacks. *J. Glaciol.*, **55**(191), 485–498 (doi: 10.3189/002214309788816687)

Wang M and 6 others (2012) The influence of dust on quantitative measurements of black carbon in ice and snow when using a thermal optical method. *Aerosol Sci. Technol.*, **46**(1), 60–69 (doi: 10.1080/02786826.2011.605815)

Warren SG (1982) Optical properties of snow. *Rev. Geophys.*, **20**(1), 67–89 (doi: 10.1029/RG020i001p00067)

Warren SG and Clarke AD (1990) Soot in the atmosphere and snow surface of Antarctica. *J. Geophys. Res.*, **95**(D2), 1811–1816 (doi: 10.1029/JD095iD02p01811)

Warren SG and Wiscombe WJ (1980) A model for the spectral albedo of snow. II. Snow containing atmospheric aerosols. *J. Atmos. Sci.*, **37**(12), 2734–2745 (doi: 10.1175/1520-0469(1980)037<2734:AMFTSA>2.0.CO;2)

Wiscombe WJ and Warren SG (1980) A model for the spectral albedo of snow. I. Pure snow. *J. Atmos. Sci.*, **37**(12), 2712–2733 (doi: 10.1175/1520-0469(1980)037<2712:AMFTSA>2.0.CO;2)

Xu B and 11 others (2009) Black soot and the survival of Tibetan glaciers. *Proc. Natl Acad. Sci. USA (PNAS)*, **106**(52), 22 114–22 118 (doi: 10.1073/pnas.0910444106)

Xu B, Cao J, Joswiak DR, Liu X, Zhao H and He J (2012) Post-depositional enrichment of black soot in snow-pack and accelerated melting of Tibetan glaciers. *Environ. Res. Lett.*, **7**(1), 014022 (doi: 10.1088/1748-9326/7/1/014022)